


## RESEARCH ARTICLE OPEN ACCESS

# Novel Transgenic Zebrafish Lines to Study the CHRNA3-B4-A5 Gene Cluster

Yuanqi Hua<sup>1</sup> | Judith Habicher<sup>1,2</sup> | Matthias Carl<sup>2</sup> | Remy Manuel<sup>1</sup> | Henrik Boije<sup>1</sup> 

<sup>1</sup>Department of Immunology, Genetics and Pathology, Uppsala University, Uppsala, Sweden | <sup>2</sup>Department of Cellular, Computational and Integrative Biology (CIBIO), University of Trento, Trento, Italy

**Correspondence:** Henrik Boije ([henrik.boije@igp.uu.se](mailto:henrik.boije@igp.uu.se))

**Received:** 12 March 2024 | **Revised:** 13 September 2024 | **Accepted:** 5 November 2024

**Funding:** Financial support was provided by: the Kjell and Marta Beijers Foundation, the Jeansson's Foundation, the Carl Tryggers Foundation, the Swedish Brain Foundation, the Swedish Research Council, the Magnus Bergvalls Foundation, the Royal Swedish Academy of Sciences, the Ake Wibergs Foundation, Olle Engkvist Stiftelse, the Ragnar Söderberg Foundation, Swedish Foundation for Strategic Research, and Swedish Research Council (Grants 2015-03359 and 2020-00943).

**Keywords:** acetylcholine (ACh) | *Danio rerio* | nervous system | nicotinic acetylcholine receptors (nAChRs) | spinal cord

## ABSTRACT

Acetylcholine (ACh), a vital neurotransmitter for both the peripheral (PNS) and central nervous systems (CNS), signals through nicotinic ACh receptors (nAChRs) and muscarinic ACh receptors (mAChR). Here, we explore the expression patterns of three nAChR subunits, *chrna3*, *chrnb4*, and *chrna5*, which are located in an evolutionary conserved cluster. This close genomic positioning, in a range of vertebrates, may indicate co-functionality and/or co-expression. Through novel transgenic zebrafish lines, we observe widespread expression within both the PNS and CNS. In the PNS, we observed expression of *chrna3*<sup>tdTomato</sup>, *chrnb4*<sup>eGFP</sup>, and *chrna5*<sup>tdTomato</sup> in the intestinal enteric nervous system; *chrna5*<sup>tdTomato</sup> and *chrnb4*<sup>eGFP</sup> in sensory ganglia of the lateral line; and *chrnb4*<sup>eGFP</sup> in the ear. In the CNS, the expression of *chrnb4*<sup>eGFP</sup> and *chrna5*<sup>tdTomato</sup> was found in the retina, all three expressed in diverse regions of the brain, where a portion of *chrna3*<sup>tdTomato</sup> and *chrnb4*<sup>eGFP</sup> cells were found to be inhibitory efferent neurons projecting to the lateral line. Within the spinal cord, we identify distinct populations of *chrna3*<sup>tdTomato</sup>-, *chrnb4*<sup>eGFP</sup>-, and *chrna5*<sup>tdTomato</sup>-expressing neurons within the locomotor network, including *dmrt3a*-expressing interneurons and *mnx1*-expressing motor neurons. Notably, three to four primary motor neurons per hemisegment were labeled by both *chrna3*<sup>tdTomato</sup> and *chrnb4*<sup>eGFP</sup>. Interestingly, we identified an sl-type secondary motor neuron per hemisegment that strongly expressed *chrna5*<sup>tdTomato</sup> and co-expressed *chrnb4*<sup>eGFP</sup>. These transgenic lines provide insights into the potential roles of nAChRs within the locomotor network and open avenues for exploring their role in nicotine exposure and addiction in a range of tissues throughout the nervous system.

## 1 | Introduction

Acetylcholine (ACh) is a key neurotransmitter, which signals through the nicotinic ACh receptors (nAChRs), located on the postsynaptic membrane (Takahashi 2020), resulting in membrane depolarization (Carlson and Kraus 2024). In vertebrates,

there are two main types of nAChRs: (1) the peripheral or muscle-type, which makes up the neuromuscular junction on skeletal muscle and is involved in muscle contraction, and (2) the neuronal-type, which are widely expressed in the peripheral (PNS) and central nervous systems (CNS). These ligand-gated ion channels are heteropentamers where muscle nAChRs are formed

Remy Manuel and Henrik Boije contributed equally.

This is an open access article under the terms of the [Creative Commons Attribution-NonCommercial-NoDerivs](https://creativecommons.org/licenses/by-nc-nd/4.0/) License, which permits use and distribution in any medium, provided the original work is properly cited, the use is non-commercial and no modifications or adaptations are made.

© 2024 The Author(s). *Developmental Neurobiology* published by Wiley Periodicals LLC.

by 5 subunits:  $\alpha 1$ ,  $\beta 1$ ,  $\delta$ ,  $\gamma$ , and  $\epsilon$ , whereas neuronal nAChRs are made up by 12 homologous neuronal nAChR subunits: 9  $\alpha$ -subunits ( $\alpha 2$ –10) and 3  $\beta$ -subunits ( $\beta 2$ –4) (Kalamida et al. 2007; Albuquerque et al. 2009). The resulting receptors, comprising different subunit combinations, have highly variable kinetic, electrophysiological, and pharmacological properties in response to ACh (Dani 2015; Zoli, Pistillo, and Gotti 2015; McGehee and Role 1995).

During development, ACh-signaling is essential for the formation of the PNS and CNS (Dwyer, McQuown, and Leslie 2009; Holbrook 2016). As foretold by its name, nicotine binds nAChRs with high affinity, and nicotine exposure during early development interferes with ACh-signaling and results in neurobehavioral and locomotor defects (Svoboda, Vijayaraghavan, and Tanguay 2002). Regarding nicotine addiction, the  $\alpha 3 \beta 4$  receptor variant plays a crucial role in reinforcing the effects (Glick et al. 2002; Perry et al. 2002), and co-assembly with the  $\alpha 5$  subunit greatly increases receptor desensitization in response to nicotine (Wang et al. 1996; Stolerman et al. 2000; Stella and Piomelli 2001). Interestingly, the genes encoding these three subunits are located in an evolutionary conserved cluster (CHRNA5-A3-B4), and single-nucleotide polymorphisms (SNPs) within this cluster have been associated with increased risk for nicotine dependency (Raimondi et al. 1992; Saccone et al. 2009; Improgo et al. 2010). Given that many of these SNPs were found in cis-regulatory elements known to regulate transcription of these genes (Xu, Scott, and Deneris 2006; Scofield, Tapper, and Gardner 2010), suggests that altered expression of these genes underlies nicotine dependency. Indeed, the balance between these subunits has been shown to play a role in nicotine addiction (Frahm et al. 2011), where deletion of the  $\alpha 5$  subunit (Fowler et al. 2011), or overexpression of the  $\beta 4$  subunit, enhanced nicotine self-administration (Yang et al. 2019).

The genes in this cluster have also been associated with the development of the locomotor network. For instance, missense variants in the CHRNA3 or CHRNA4 gene have been linked to sporadic amyotrophic lateral sclerosis, a motor neuron degenerative disease in humans (Sabatelli et al. 2009). Thus, SNPs within the CHRNA5-A3-B4 cluster could potentially increase the risk for locomotor defects. A previous study regarding ethanol-induced locomotor activity (Kamens et al. 2009) revealed that *Chrna3*(+/-) mice exhibit greater locomotor depression. A recent study, using in situ hybridization, revealed the expression of *chrna3* within the zebrafish spinal locomotor network (Rima et al. 2020). However, the expression patterns of *chrna5* and *chrnb4* within the zebrafish spinal cord are unknown.

We set out to explore the expression of the *chrna3-b4-a5* cluster in the nervous system by generating transgenic reporter lines: Tg(*chrna3*:hs:tdTomato), Tg(*chrnb4*:hs:eGFP), Tg(*chrna5*:hs:tdTomato), and Tg(*chrna5*:hs:eGFP). Over development, we observed expression in distinct areas of the PNS (e.g., the gastrointestinal tract, ear, and lateral line sensory ganglia) and in the CNS (e.g., eye, olfactory bulb [OB], habenula, pineal gland, optic tectum, rhombencephalon, and the spinal cord). Using previously published transgenic lines, we were able to identify some of the cells in the rhombencephalon as inhibitory efferent neurons projecting to the lateral line. Quantification of spinal neurons showed co-expression of *chrnb4*<sup>eGFP</sup> with *chrna3*<sup>tdTomato</sup> and *chrna5*<sup>eGFP</sup>. On the basis

of calculations, a portion of neurons likely co-express all three *chrn*-genes. We found expression of all three *chrn*-genes within *dmrt3a*-expressing interneurons and *mx1a*-expressing motor neurons. All primary motor neurons (pMN) expressed *chrnb4*<sup>eGFP</sup> and *chrna3*<sup>tdTomato</sup>, but only a single primary motor neuron per segment expressed *chrna5*<sup>eGFP</sup>. Moreover, one type of secondary motor neuron, identified as sI-type, strongly expressed *chrna5*<sup>tdTomato</sup>. Although our study is limited to the characterization of the expression by this gene cluster, it could serve as a steppingstone for further studies. For instance, investigations regarding expression profiles correlated to the distinct speed modules previously described in zebrafish (McLean and Fetcho 2009). These transgenic lines also open doors to investigating the intricate interplay between genetics, development, behavior, and environmental factors.

## 2 | Materials and Methods

### 2.1 | Animals and Husbandry

Zebrafish (*Danio rerio*) used in this study were kept at Genome Engineering Zebrafish National Facility (SciLifeLab, Uppsala, Sweden) under the standard conditions of 14 h light/10 h dark cycles at 28°C. The embryos and larvae used during the study were kept in water with methylene blue and housed under constant darkness at 28°C. Larvae from stable transgenic lines used for imaging were treated with 1-phenyl-2-thiourea (PTU, 0.003% final concentration) at 24 h post-fertilization (hpf) to avoid pigment formation. The housing and manipulation of zebrafish were following the local welfare standards and the European Union legislation (EU-Directive 201\_63).

### 2.2 | Transgenic Lines

The following pre-existing transgenic lines were used: Tg(*dmrt3a*:Gal4;UAS:GFP) (Satou et al. 2013), Tg(UAS:RFP) (Dr. Kaska Koltowska, Uppsala University, Sweden), and Tg(*mx1*:Gal4) (Seredick et al. 2012). We generated Tg(*chrna3*:hs:tdTomato), Tg(*chrnb4*:hs:eGFP), Tg(*chrna5*:hs:eGFP), and Tg(*chrna5*:hs:tdTomato) specifically for this study, using the CRISPR/Cas9-knock-in method described by Kimura et al. (2014).

### 2.3 | sgRNA Template Assembly

Template assembly was done according to Habicher et al. (2022). Using the oligo assembly approach to prepare sgRNAs, we synthetically added a G where sequences did not start with GG, as this is crucial for the T7 polymerase. We designed the following Oligo A sequences (T7-Genomic sequence):

*chrna3*: “taatacagactcactata-GGAAGACGAACGATCGTCATgttttagagctagaatagcaag,”

*chrnb4*: “taatacagactcactata-GGGAGCGCTCGGACCGGCGGgttttagagctagaatagcaag,” and

*chrna5*: “taatacagactcactata-GGGCGGGAAAATGCAAGGAGgttttagagctagaatagcaag.”

The oligos were then annealed with a second fragment containing the guide core sequence (oligoB; Varshney et al. 2015). PCR was performed under the following conditions: 2 min, 98°C for denaturation; 10 min, 50°C for annealing; 10 min, 72°C.

## 2.4 | Genomic sgRNA and Cas9 mRNA Synthesis and Purification

The templates were used for RNA in vitro transcription with the mMESSAGE mMACHINE T7 Transcription Kit (Invitrogen, AM1344) and incubated overnight at 37°C. DNA template was removed by incubating for 15 min at 37°C with DNase I (Thermo Fisher Scientific).

To prepare Cas9 mRNA, pT3Ts-nCas9 plasmid (Addgene #46757) was digested with XbaI (NEB), purified, and used for T3-driven in vitro transcription according to the manual provided by the manufacturer (mMESSAGE mMACHINE T3 Kit, Life Technologies). Purification of sgRNA and Cas9 mRNA was done using the GeneJET RNA Cleanup and Concentration Micro kit (Thermo Fisher Scientific, K0841). The final product was stored at -80°C.

## 2.5 | Generation of Transgenic Lines

Eggs used for the injections were obtained from group breeding of AB wild-type fish. Glass capillaries (Harvard Apparatus, GC 100FS-10) were pulled (Sutter Instrument, model P-1000) for injection needles. The insertion of hs:tdTomato or hs:eGFP in the 5' UTR of the gene was done by injecting 1 nL of plasmid mix (1.0 µL mbait-hs:tdTomato or mbait-hs:eGFP plasmid [1000 ng/µL], 1.5 µL Cas9 mRNA [750 ng/µL], 2.5 µL Cas9 protein [1000 ng/µL], 2.0 µL genomic sgRNA [250 ng/µL], 2.0 µL Mbait sgRNA [250 ng/µL], 1.0 µL phenol red dye [0.075%]) into the cell of one-cell stage embryos. Injected embryos were screened at 3–5 days post fertilization (dpf) for tdTomato- or eGFP-positive cells in the nervous system via a fluorescent stereomicroscope (Leica, MZ10F). Positive larvae were grown and screened for germline transmission at 3 months.

## 2.6 | PCR

PCR was performed to verify the location and direction of insert. We designed two primers against the genomic sequence of *chrna3*, *chrnb4*, and *chrna5* and paired these with a single primer against the heat shock promoter (hs) present in the knock-in construct, acting as either forward or reverse (GCCCGTCTGTTTCATTGTTTT). For forward insertion, we used *chrna3* forward primer TCGGGTGGTTTCATGTGTGT, *chrnb4* forward primer ATGTGTTGATATAAACTGTCTGCAT, and *chrna5* forward primer GCACAGTTCCTCATCAA. For the reverse insertion, we used *chrna3* reverse primer TGGAGAGCTCCGGTGTTCATT, *chrnb4* reverse primer TCCTCATCAATGCTGTTGGC, or *chrna5* reverse primer GATTGGCATGGACACACGAC.

Single larvae at 5 dpf were dissolved in 30 µL 50 mM NaOH for 20 min at 95°C, followed by the addition of 60 µL 50 mM Tris-HCl to extract DNA. PCR was used to amplify the targeted sequence

with the following cycle conditions: 3 min at 95°C; 30 s at 95°C; 30 s at 60°C; 1 min at 72°C (cycling for 35 times); and 90 s at 72°C. Samples were loaded on agarose gel (1.5%) to check for product.

## 2.7 | Whole-Mount In Situ Hybridization

RNA was extracted from zebrafish embryos and larvae at different stages using Trizol, and reverse transcription was performed using a reverse transcriptase (Super Script II, Invitrogen). The cDNA was then used as a template for the PCR with 95°C for 5 min, 34 cycles of: 95°C for 30 s, 60°C for 1 min, 72°C for 30 s, and finally, 72°C for 5 min. The following primers were used: 5-AAGTTTGGCTCGTGGACCTA-3 and 5-CGCTGGTCATGTTGGAGATG-3 for *chrna3*, 5-ATCAGGGTGCCTTCAGACTC-3 and 5-AGAGCAGTCTAGGC AAGTGG-3 for *chrna5*, and 5-CAGAAGTGCACGCTCAAG TT-3 and 5-TACAGCCTGTTCCTTCAG-3 for *chrnb4*. In addition, a T7 overhang (CTGTAATACGA CTTACTATAGGG) was added to the reverse primer, and therefore the PCR products could be directly used for purification with Qiagen PCR purification kit and then transcription of the RNA probe using the T7 polymerase (Thermo Scientific) and digoxigenin RNA labeling kit (Roche).

In situ hybridization was generally performed according to standard procedures (Thisse and Thisse 2008). In short, zebrafish embryos and larvae were fixed with 4% paraformaldehyde (PFA) at different stages of development and stored in 100% methanol at -20°C. Rehydration and permeabilization in Proteinase K were followed by refixation with 4% PFA. After that, digoxigenin-labeled RNA probes were incubated overnight in a water bath at 65°C. Next day, careful washings were followed by incubation with anti-dig FAB fragments at 4°C overnight. On the last day, washing was followed by a colorimetric reaction using BM Purple AP Substrate (Roche). Stained larvae were embedded in glycerol and imaged using a Zeiss Axio Imager M2 microscope in brightfield mode using 10× and 20× objectives.

## 2.8 | Microscopy

A Leica SP8 confocal microscope (Leica Microsystems, Wetzlar, Germany) was used for characterization of transgenic lines. The larvae were anesthetized with tricaine (0.12 mg/mL), embedded in low melting point agarose (1.2%), and imaged using a 25× water objective. Leica's LasX software and Fiji were used for image processing and analysis.

## 3 | Results and Discussion

To explore the expression pattern of *chrna3*, *chrnb4*, and *chrna5* during zebrafish development, transgenic reporter lines were generated using CRISPR/Cas9-mediated knock-in (Kimura et al. 2014; Habicher et al. 2022). PCR analysis was used to confirm the location and orientation of the inserted construct (Figure S1). For consistency, all imaging data for Tg(*chrna3*:hs:tdTomato) are shown in cyan, Tg(*chrnb4*:hs:eGFP) in green, and Tg(*chrna5*:hs:tdTomato) and Tg(*chrna5*:hs:eGFP) in magenta. We observed expression of the reporter genes in the

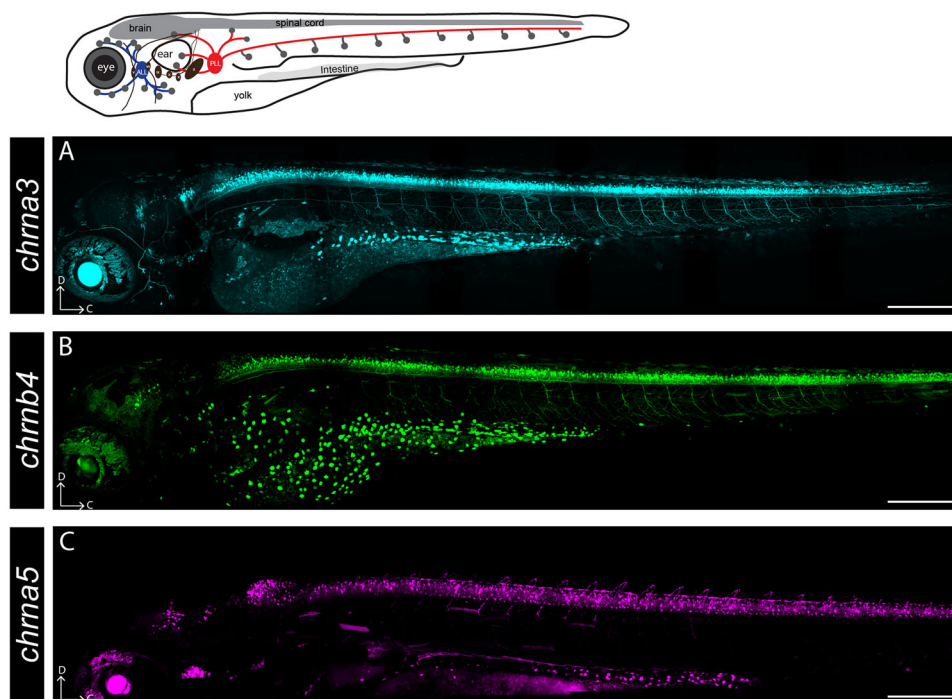


**FIGURE 1** | Overview of the expression of *chrna3*<sup>tdTomato</sup>, *chrnb4*<sup>eGFP</sup>, and *chrna5*<sup>tdTomato</sup> at 5 dpf. (A–C) Lateral view of the zebrafish larvae labeled by *chrna3* (cyan) *chrnb4* (green) and *chrna5* (magenta) expression. Scale bars equal 250  $\mu\text{m}$ . C, caudal; D, dorsal.

intestine, the eyes and ear, cranial sensory ganglia, the brain, and spinal cord at 5 dpf (Figure 1).

### 3.1 | Expression in the PNS and the Eye

#### 3.1.1 | The Intestine

Expression of *chrna3*<sup>tdTomato</sup>, *chrnb4*<sup>eGFP</sup>, and *chrna5*<sup>tdTomato</sup> was observed in the zebrafish intestine (Figure 2A–C). On the basis of distribution and morphology of the positive cells, they are likely part of the enteric nervous system (Kuil et al. 2021), which regulates local gut functions and is known to express *Chrna3-b4-a5* in rodents (Garza et al. 2009) and humans (Rueda Ruzafa, Cedillo, and Hone 2021).

#### 3.1.2 | The Ear and Eye

We observed *chrnb4*<sup>eGFP</sup> expression in the otic capsule (ear; Figure 2D). On the basis of the inner ear structure of zebrafish, we speculate that these *chrnb4*<sup>eGFP</sup>-expressing cells are in the region of the semicircular canal crista ampullaris (Baeza-Loya and Raible 2023). This observation is in line with expression in mice, where *Chrnb4* is expressed in the inner ear (Gabashvili et al. 2007) and in the chicken otic vesicle that expresses *CHRN4*, but not *CHRNA3* (Patthey et al. 2016).

For the eye, we found expression of *chrnb4*<sup>eGFP</sup> in the ganglion cell layer (GCL), the inner nuclear layer (INL), and the outer nuclear layer (ONL; Boije et al. 2015). In contrast, *chrna5*<sup>tdTomato</sup> expression was only found in the ONL (Figure 2E–G), whereas we observed no *chrna3*<sup>tdTomato</sup> expression in the retina. The presence

of *chrnb4* and *chrna5* in the retina is in line with recent zebrafish single-cell data (Sur et al. 2023). Expression of *Chrn4* has also been described in the mouse retina (Decembrini et al. 2017).

#### 3.1.3 | The Facial Sensory Ganglion

We found *chrnb4*<sup>eGFP</sup> and *chrna5*<sup>tdTomato</sup> cells, but not *chrna3*<sup>tdTomato</sup> cells, in the sensory ganglia of the head (Figure 2H,I). We were able to identify positive cells in the following four cranial nerves, all of which carry both sensory and motor information: the trigeminal (V), facial (VII), glossopharyngeal (IX), and vagal (X) nerves (LaMora and Voigt 2009). In addition, we found positive cells in the anterior and posterior sensory ganglia of the lateral line (Bleckmann and Zelik 2009). Many of the sensory ganglia in humans, including the jugular and nodose ganglia, also express *CHRN4* and *CHRNA5* (Rueda Ruzafa, Cedillo, and Hone 2021). Similarly, a number of cells in the mouse spiral ganglia of the ear were found to express *Chrn4* (Shrestha et al. 2018). Of note, in mammals, the expression of the *chrn*-genes has also been described in the dorsal root ganglia of the spinal cord (Lee, Barrie, and Sadee 2019). However, we were unable to detect any expression of our reporter genes in the dorsal root ganglia of 5 dpf zebrafish larvae.

### 3.2 | Expression in the CNS

#### 3.2.1 | Inhibitory Efferent Neurons of the Lateral Line

We found the expression of *chrna3*<sup>tdTomato</sup> and *chrnb4*<sup>eGFP</sup>, but not *chrna5*<sup>tdTomato</sup>, in the inhibitory efferent neurons of the lateral

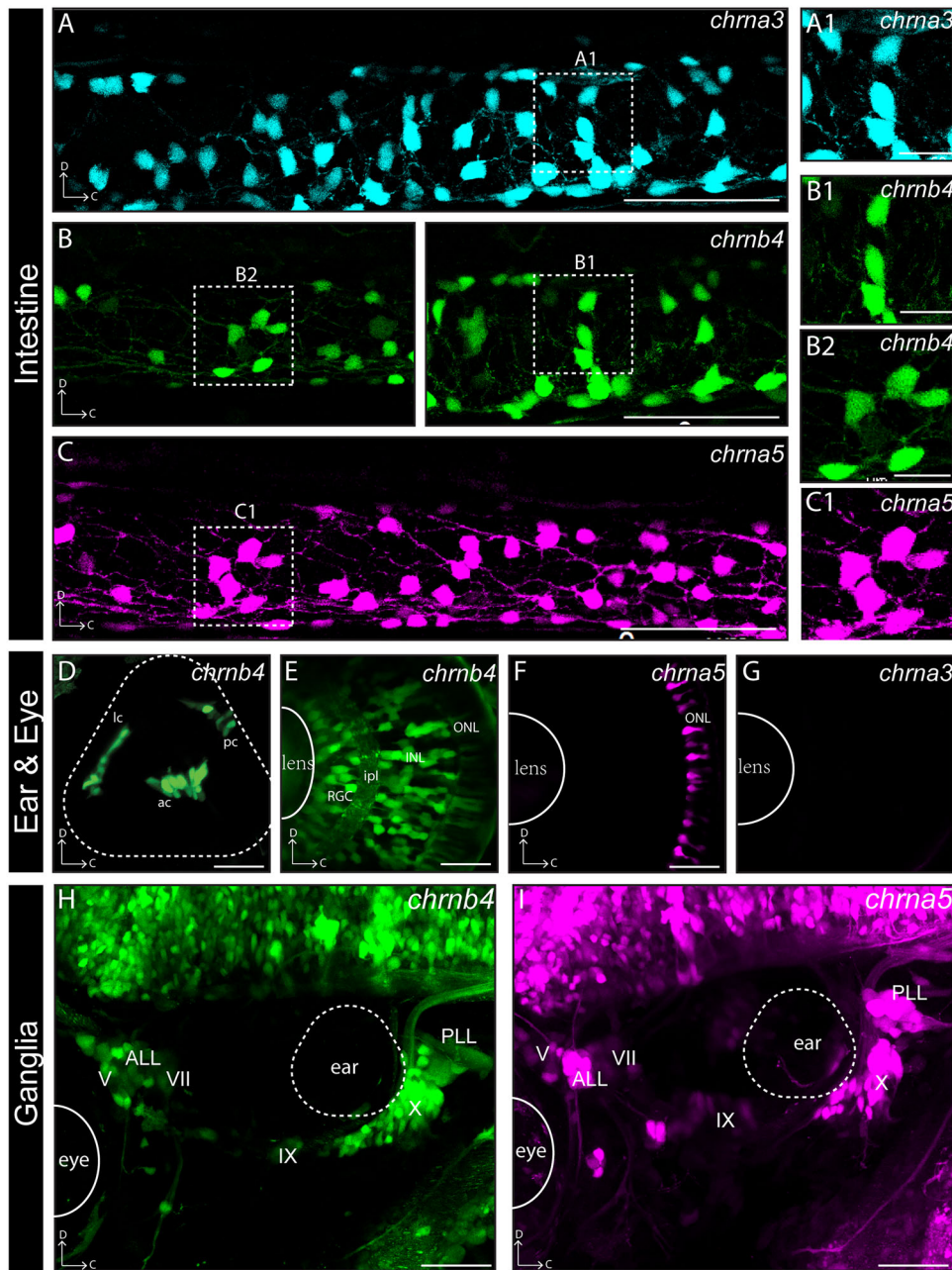


**FIGURE 2** | Expression of *chrna3*<sup>tdTomato</sup>, *chrnb4*<sup>eGFP</sup>, and *chrna5*<sup>tdTomato</sup> in the peripheral nervous system and eyes. (A–C) Lateral view of the intestine of zebrafish larvae at 5 dpf. (A1–C1) Zoom images of marked regions in (A)–(C). (D) Lateral view of the ear labeled by *chrnb4*<sup>eGFP</sup>. Dashed circles refer to the outline of ear. (E and F) Lateral view of the eye labeled by *chrnb4*<sup>eGFP</sup> and *chrna5*<sup>tdTomato</sup>. (G) Lateral view of the eye of transgenic fish of *chrna3*<sup>tdTomato</sup>. (H and I) Lateral view of the head labeled by *chrnb4*<sup>eGFP</sup> and *chrna5*<sup>tdTomato</sup> at 3 dpf revealed the expression in the sensory ganglia, including the trigeminal (gV), facial (gVII), glossopharyngeal (gIX), vagal (gX) ganglia, and both anterior (ALL) and posterior (PLL) ganglia of lateral line. Scale bars equal 60  $\mu$ m in (A)–(C), 20 in (A1)–(C1), 30 in (D)–(G), 50  $\mu$ m in (H) and (I). ac, anterior crista; C, caudal; D, dorsal; INL, inner nuclear layer; ipI, inner plexiform layer; Lc, lateral crista; ONL, outer nuclear layer; pc, posterior crista; RGC, retinal ganglion cell.

line (Figure 3A–C). To verify if the *chrn*-genes were expressed in all inhibitory efferent neurons, we crossed our lines with Tg(*dmrt3a*:Gal4, UAS:RFP) or Tg(*dmrt3a*:Gal4, UAS:GFP), which labels all the inhibitory efferent neurons (Manuel et al. 2021). The distinct axonal projections in the brain revealed an overlap, and tracing the projections to the level of the neuromast revealed a complete overlap in all larvae studied (Figure 3D,E). These observations suggest that all of the lateral line inhibitory efferent neurons express *chrna3* and *chrnb4*.

### 3.2.2 | Expression in the Brain

Previously, studies including in situ hybridization, multiple tissue expression array analysis, immunopurification, or immunoprecipitation revealed expression of *Chrna3*, *Chrnb4*, and *Chrna5* in the OB, optic tectum (TeO), cerebellum (Ce), and hindbrain (Hb; Dineley-Miller and Patrick 1992; Flora et al. 2000; Grady et al. 2009; Hellström-Lindahl et al. 1998; Moretti et al. 2004; Winzer-Serhan and Leslie 1997; Zoli et al. 1995; Grady et al. 2009;

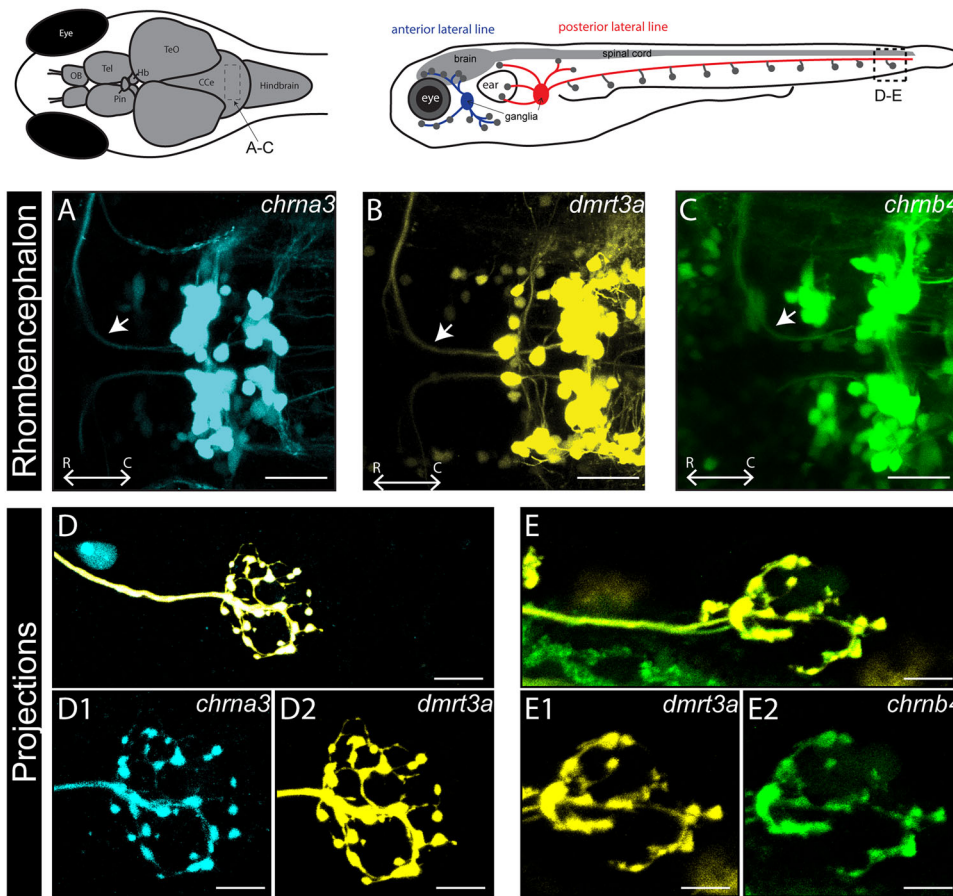


**FIGURE 3** | Expression of *chrna3*<sup>tdTomato</sup>, *chrnb4*<sup>eGFP</sup>, and *chrna5*<sup>tdTomato</sup> in efferent neurons projecting to the lateral line. (A–C) Dorsal view of the hindbrain of *chrna3*<sup>tdTomato</sup>, *chrnb4*<sup>eGFP</sup>, as well as *dmrt3*<sup>tdTomato</sup> expressed in the region where CEN and REN located and the inhibitory efferent axon (arrow) sent out by these cells. (D and E) Projections of *chrna3*<sup>tdTomato</sup> and *chrnb4*<sup>eGFP</sup> overlapped with *dmrt3a*<sup>eGFP</sup> or *dmrt3a*<sup>RFP</sup> at the level of neuromasts of the anterior and posterior lateral lines. Scale bars equal 30  $\mu$ m in (A)–(C), 10  $\mu$ m in (D) and (E). C, caudal; R, rostral.

Lein et al. 2007). Building on this, our exploration of the brain allowed us to identify cells expressing the *chrn*-genes in these regions of the brain (Figure 4A–C). Expression in the forebrain was seen in the OB, pineal gland, habenula, and telencephalon. Midbrain expression included the optic tectum, and hindbrain expression was seen in the corpus cerebellum. In support of these observations, we performed in situ hybridization against *chrna3*, *chrnb4*, and *chrna5* and observed staining of regions similar to those marked in our transgenic lines (Figure S2A–C). For the pineal gland and the optic tectum, higher magnification images were used to identify the *chrn*-positive cells.

The pineal gland mainly comprises three types of cells: photoreceptor cells, projection neurons, and interstitial cells (Shainer et al. 2017). On the basis of morphological characteristics, such as a large soma and distinct projections (Li et al. 2012), we were able to identify some of the cells as double-cone photoreceptor cells (Figure 4A1, B1, C1).

In the optic tectum, we found that *chrna3*<sup>tdTomato</sup>-, *chrnb4*<sup>eGFP</sup>-, and *chrna5*<sup>tdTomato</sup>-expressing cells were distributed throughout the stratum periventricular (SPV), which contains the cell bodies of most tectal neurons, whose axons project to the tectal neuropil (Figure 4A2, B2, C2). As the projections of *chrna3*<sup>tdTomato</sup>-, *chrnb4*<sup>eGFP</sup>-, and *chrna5*<sup>tdTomato</sup> cells were seen throughout the

entire neuropil, we propose that all four types of tectal neurons were labeled, that is, those with non-stratified, mono-stratified, bistratified, and tristratified dendritic arbors (Folgueira et al. 2007; DeMarco et al. 2020; Förster et al. 2020).

### 3.3 | Expression in the Spinal Cord

In the spinal cord, *chrna3*<sup>tdTomato</sup>-, *chrnb4*<sup>eGFP</sup>-, and *chrna5*<sup>tdTomato</sup>-expressing cells were widely distributed (Figure 5A–C). The *chrna3*<sup>tdTomato</sup> cells were predominantly located at the center of the dorsal–ventral axis of the spinal cord and spread evenly along the medial–lateral axis. Whereas the *chrna3*<sup>tdTomato</sup> cells form a “layer” (Figure 5A3), the *chrnb4*<sup>eGFP</sup> cells appear throughout the entire spinal cord (Figure 5B3). The *chrna5*<sup>tdTomato</sup> cells were distributed across the entirety of the dorsal–ventral axis of the spinal cord but were restricted medially in the dorsal region and laterally in the ventral region (Figure 5C3). We observed a similar distribution in our in situ hybridization against *chrna3*, *chrnb4*, and *chrna5*, where we saw strong staining dorsally for *chrna3* and ventrally for *chrna5* (Figure S2A–C).

We quantified the number of *chrna3*<sup>tdTomato</sup>-, *chrnb4*<sup>eGFP</sup>-, and *chrna5*<sup>tdTomato</sup> cells in 1–5 dpf old larvae. For all *chrn*-genes, as development progressed, the fluorescent reporters became

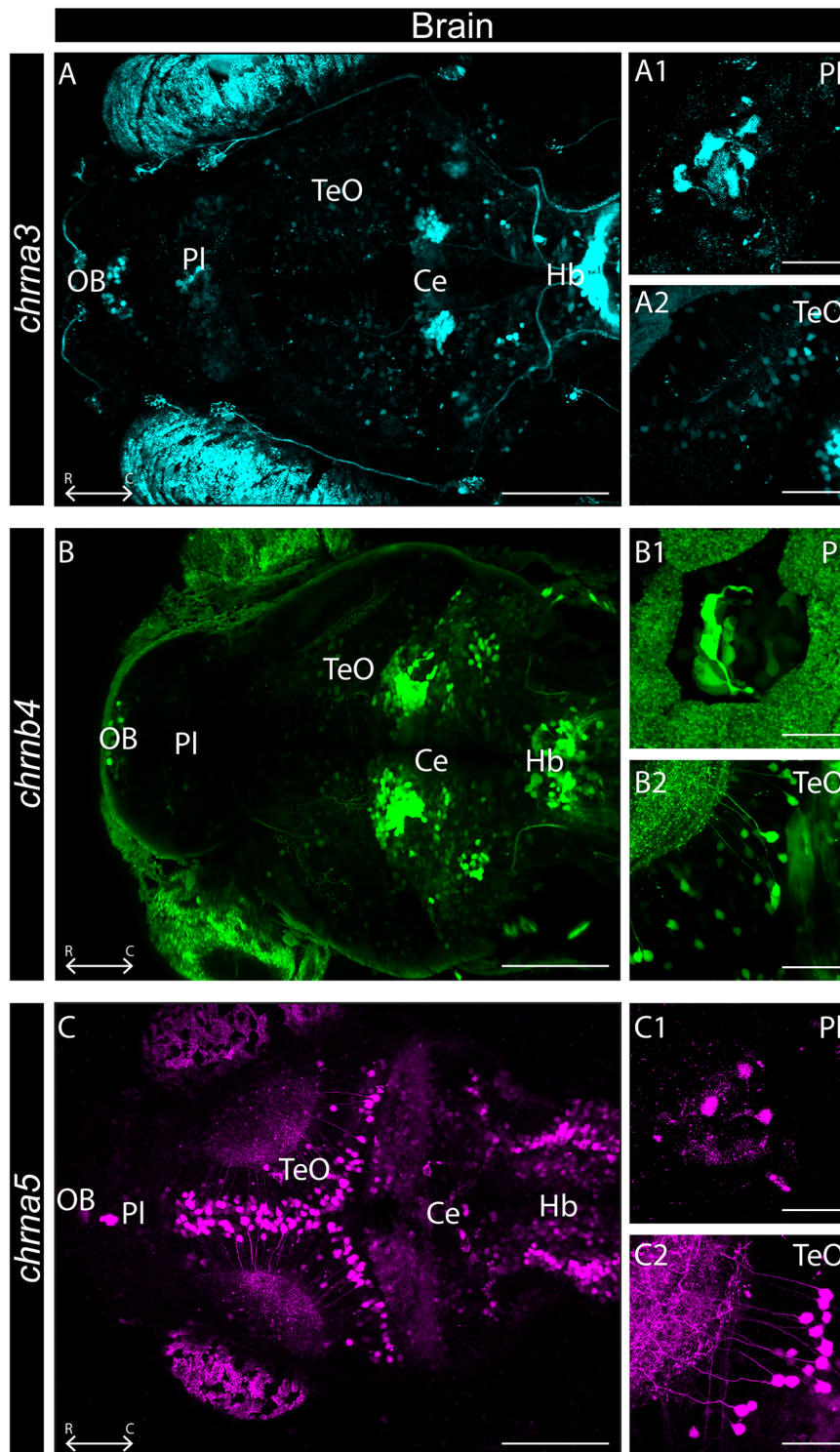


**FIGURE 4** | Expression of *chrna3*<sup>tdTomato</sup>, *chrnb4*<sup>eGFP</sup>, and *chrna5*<sup>tdTomato</sup> in the brain at 5 dpf. (A–C) Dorsal view of the expression of *chrna3*<sup>tdTomato</sup>, *chrnb4*<sup>eGFP</sup>, and *chrna5*<sup>tdTomato</sup> in the brain. (A1–C1) dorsal view of the pineal gland (PI). (A2–C2) Dorsal view of the optic tectum (TeO). Scale bars equal 100  $\mu$ m in (A)–(C), 20  $\mu$ m in (A1)–(C1). C, caudal; Ce, cerebellum; Hb, hindbrain; OB, olfactory bulb; R, rostral.

more apparent, suggesting either an increase in expression or a continuation of expression within the cells. The peak number of cells for *chrna3*<sup>tdTomato</sup> ( $64.4 \pm 1.5$  cells/segment,  $n = 5$  larvae) and *chrnb4*<sup>eGFP</sup> ( $159.4 \pm 3.63$  cells/segment,  $n = 5$  larvae) were at 3 dpf, and for *chrna5*<sup>tdTomato</sup> ( $154.4 \pm 20.01$  cells/segment,  $n = 5$  larvae) at 4 dpf (Figure 5D).

### 3.3.1 | Co-Expression of chrn-Genes

Next, we quantified the number of cells that co-express the chrn-genes at 5 dpf (Figure 5E–H). We focused on the *chrna3*<sup>tdTomato</sup> population ( $64.4 \pm 1.5$  cells/segment,  $n = 5$  larvae), as this was the smallest among the three. Here, we found that  $38.6 \pm 1.2$  cells

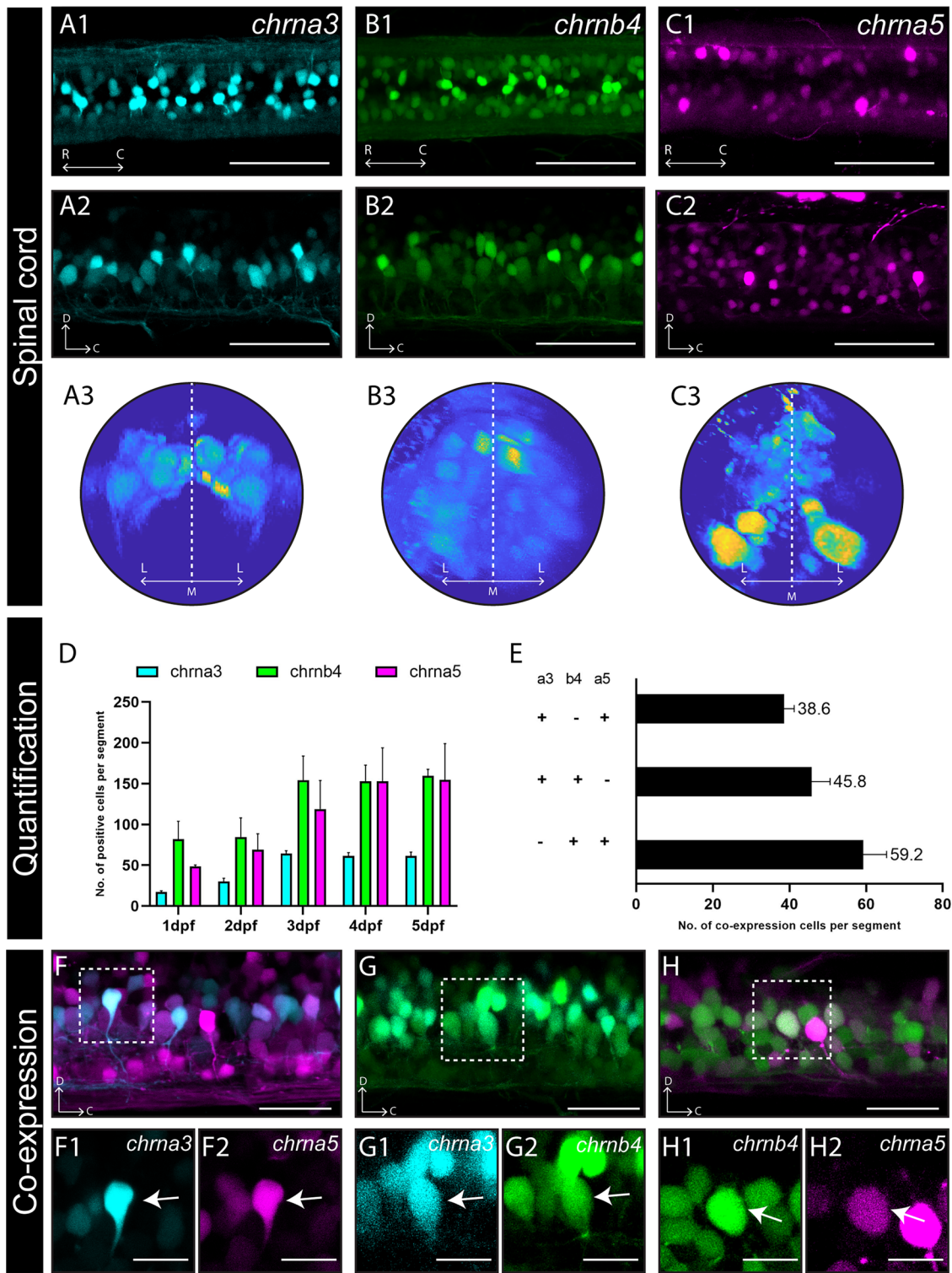


**FIGURE 5** | Expression of *chrna3*<sup>tdTomato</sup>, *chrnb4*<sup>eGFP</sup>, and *chrna5*<sup>tdTomato</sup> in the spinal cord. (A1–C1) Dorsal view of the spinal cord of each transgenic line. (A2–C2) Lateral view of the spinal cord of each transgenic line. (A3–C3) Transverse view of the spinal cord of each transgenic line, color gradient represents levels of fluorescence (yellow = stronger/blue = weaker). (D) Quantification of positive cells per segment was counted from Days 1 to 5,  $n = 5$  fish for each transgenic line. (E) Quantification of co-expressing cells in the spinal cord. The number of positive cells per segment in the spinal cord was counted at 5 dpf,  $n = 5$  fish for each combination. (F–H) Lateral view of spinal cord showed the co-expression of *chrna3*<sup>tdTomato</sup> and *chrna5*<sup>tdTomato</sup>, *chrna3*<sup>tdTomato</sup>, and *chrnb4*<sup>eGFP</sup>, as well as *chrnb4*<sup>eGFP</sup> and *chrna5*<sup>tdTomato</sup>, co-expressing in the spinal cord (dashed square; arrow, overlapped cell). Scale bars equal 50  $\mu\text{m}$  in (A1)–(C2), 25  $\mu\text{m}$  in (F)–(H), 10  $\mu\text{m}$  in (F1)–(H2). Quantification data show mean values + standard deviation. C, caudal; D, dorsal; M, middle; R, rostral.



(59.9%) co-expressed *chrna5*<sup>eGFP</sup> and  $45.8 \pm 2.1$  cells (71.1%) co-expressed *chrnb4*<sup>eGFP</sup>. From these numbers, we can deduce that between 20.0 and 38.6 (31.1%–59.9%) *chrna3*<sup>tdTomato</sup>-expressing cells co-express both *chrnb4*<sup>eGFP</sup> and *chrna5*<sup>eGFP</sup> (Figure S3). On the basis of the position of the *chrna3*<sup>tdTomato</sup> cells (Figure 5A3), co-expressing cells are likely predominately interneurons. For completion, we also assessed overlap within the *chrnb4*<sup>eGFP</sup> population ( $159.4 \pm 3.6$  cells/segment,  $n = 5$  larvae) and saw that  $45.8 \pm 2.2$  cells (28.7%) co-expressed *chrna3*<sup>tdTomato</sup> and  $59.2 \pm 2.7$  cells (37.1%) co-expressed *chrna5*<sup>tdTomato</sup>. For the *chrna5*<sup>tdTomato</sup> population ( $154.4 \pm 20.01$  cells/segment,  $n = 5$  larvae), we observed that  $59.2 \pm 2.7$  cells (38.3%) co-expressed *chrnb4*<sup>eGFP</sup> and  $38.6 \pm 1.2$  cells (25.0%) of cells co-expressed *chrna3*<sup>eGFP</sup> (Figure 5E–H).

### 3.4 | Expression Within the Locomotor Network

The wide expression of *chrna3*<sup>tdTomato</sup>, *chrnb4*<sup>eGFP</sup>, and *chrna5*<sup>tdTomato</sup> in the spinal cord suggests that these receptor subtypes are used by sensory projection neurons, inhibitory and excitatory interneurons, and motor neurons. As exposure to nicotine during early development can lead to locomotor defects, we set out to gain more detailed information regarding expression in neurons, part of the locomotor network.

#### 3.4.1 | Expression Within Motor Neurons

In the hindbrain, a number of distinct *chrna5*<sup>tdTomato</sup>-positive cells were found in the region of Rhombomere 8. A cross with Tg(*mxn1*:Gal4; UAS:eGFP), marking *mxn1*-positive motor neurons in zebrafish (Seredick et al. 2012; Bello-Rojas et al. 2019), revealed co-expression, suggesting that these neurons are involved in locomotor activity (Figure 6A). These cells were also *chrnb4*<sup>eGFP</sup>-positive (Figure 6B) but did not express *chrna3*<sup>tdTomato</sup>. Although uncertain about the identity of these neurons, their location and low number make it unlikely that these neurons are branchiomotor neurons, which are more numerous and located more caudally (Chandrasekhar et al. 1997; Figure 6A, encircled). We did observe that the number of neurons is not consistent among animals, and they appear to diminish in number as the larva develops (personal observation).

We observed that a portion of *chrna3*<sup>tdTomato</sup>-, *chrnb4*<sup>eGFP</sup>-, and *chrna5*<sup>tdTomato</sup>-positive cells had axons innervating muscles, indicating that they are motor neurons. To quantify the number of motor neurons expressing our *chrn*-genes, we assessed co-expression with *mxn1*<sup>RFP/eGFP</sup> (Figure 6C–E). We found that out of  $51.6 \pm 3.8$  *mxn1*<sup>RFP/eGFP</sup> cells per segment ( $n = 5$  larvae),  $9.2 \pm 1.0$  cells (17.8%) co-expressed *chrna3*<sup>tdTomato</sup>,  $13.8 \pm 0.8$  cells (26.7%) co-expressed *chrnb4*<sup>eGFP</sup>, and  $13.4 \pm 2.5$  cells (26.0%) co-expressed *chrna5*<sup>eGFP</sup> (Figure 6F).

On the basis of soma size and position, we surmise that both primary motor neurons (pMN) and secondary motor neuron (sMN) expressed *chrna3*<sup>tdTomato</sup>, *chrnb4*<sup>eGFP</sup>, or *chrna5*<sup>eGFP</sup>. Interestingly, the expression of *chrna3* was mostly absent in motor neurons at 1 dpf (Rima et al. 2020), which suggests expression is either switched on as the network develops or is not present in the early born pMN. The pMNs, typically three to four cells per

hemisegment were identified based on their more dorsal location and larger soma (Iglesias Gonzalez et al. 2024). On average, we identified  $3.5 \pm 0.1$  pMNs per hemisegment ( $n = 5$  larvae). For these, we observed expression of *chrna3*<sup>tdTomato</sup> in  $3.3 \pm 0.1$  pMNs per hemisegment, *chrnb4*<sup>eGFP</sup> in  $3.5 \pm 0.1$  pMNs per hemisegment, and *chrna5*<sup>eGFP</sup> in  $0.9 \pm 0.2$  pMNs per hemisegment (Figure 6G). These observations suggest that all pMNs express *chrna3*<sup>tdTomato</sup>, and *chrnb4*<sup>eGFP</sup>, but only one expresses *chrna5*<sup>eGFP</sup>. The pMN types have a distinct and “fixed” positioning along the rostral–caudal axis. Our imaging data revealed that *chrna5*<sup>eGFP</sup> was predominantly expressed in the 2nd pMN (8/10), suggesting these are MiP-type pMN (Bello-Rojas et al. 2019). In the remaining cases, expression was observed in the 3rd pMN (2/10).

Interestingly, among the sMNs in each hemisegment, there was a single cell that highly expressed *chrna5*<sup>tdTomato</sup>, co-expressed *chrnb4*<sup>eGFP</sup>, but did not express *chrna3*<sup>eGFP</sup> (Figure 6H,I). This neuron is positioned ventrally and exclusively innervates superficial slow muscle fibers via the septal nerve. On the basis of this, we believe it is an sI-type sMN (Bello-Rojas et al. 2019).

#### 3.4.2 | Expression Within Interneurons

By crossing our lines to a *dmrt3a* transgenic reporter line, marking dl6 inhibitory interneurons (Satou et al. 2013; Iglesias González et al. 2021), we were able to assess (co-)expression in inhibitory interneurons of the locomotor network (Figure 7A–C). Within the spinal cord *dmrt3a*<sup>RFP/dmrt3a</sup><sup>eGFP</sup> population ( $41.0 \pm 2.3$  cells/segment,  $n = 5$  larvae), we found the co-expression of *chrna3*<sup>tdTomato</sup> in  $5.8 \pm 0.4$  cells (14.1%), *chrnb4*<sup>eGFP</sup> in  $4.8 \pm 0.4$  cells (11.7%), and *chrna5*<sup>eGFP</sup> in  $4.2 \pm 0.5$  cells (10.2%; Figure 7D). The number of *dmrt3a*<sup>RFP/dmrt3a</sup><sup>eGFP</sup> cells was in line with a previous study (Iglesias González et al. 2021), where single-cell mRNA sequencing also revealed expression of *chrna5* in some, but not all, *dmrt3a*-expressing cells.

### 3.5 | Limitations

How rigidly one validates a new transgenic reporter is tightly linked to the question at hand. Here, we wished to observe the overlapping expression patterns of these clustered homologous genes during development. The expression patterns observed in the reporter lines presented here show a high degree of correlation with previously published work. In addition, PCR analyses of the insert location of the reporter gene indicate that we have targeted the correct genes. Finally, we performed in situ hybridization against *chrna3*, *chrnb4*, and *chrna5* to highlight similarities with the transgenic line for the same gene and differences among the *chrn*-genes (Figure S2). Unfortunately, in our hands, the in situ hybridizations did not yield high-resolution results, and tissue-wide staining prevented the identification of specific regions in some cases. However, where able, we observed staining in regions corresponding to neurons marked by our transgenic lines. This, combined with the similarity to expression patterns reported in previous studies and our genomic insert verification, strongly suggest that our transgenic lines label the correct tissues and cells. Still, for functional studies of these receptor subtypes, we suggest additional approaches for validation. For instance, immunohistochemistry against the

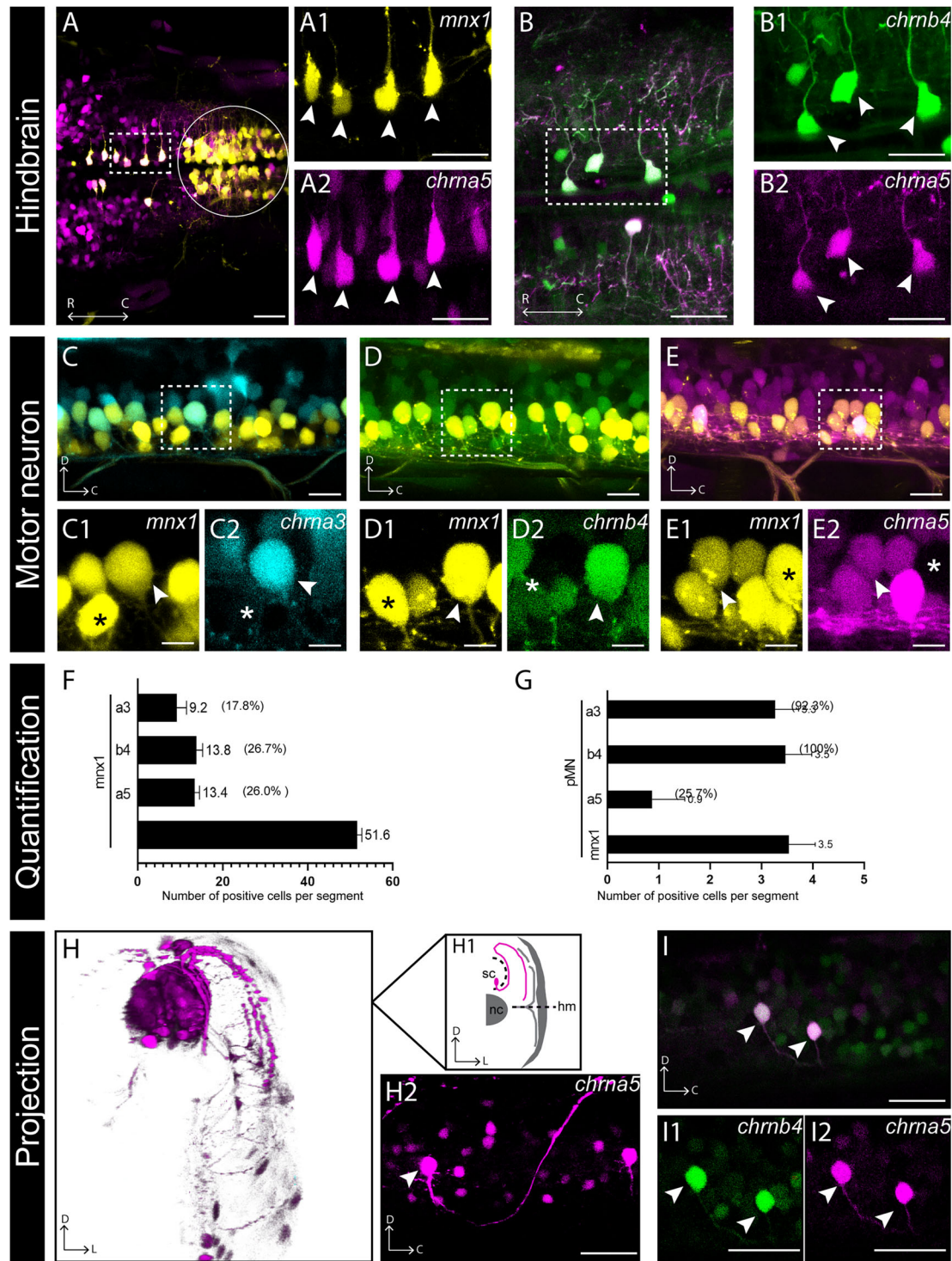


**FIGURE 6** | Expression of *chRNA3*<sup>tdTomato</sup>, *chRNB4*<sup>eGFP</sup>, and *chRNA5*<sup>tdTomato</sup> in motor neurons. (A and B) Dorsal view of the hindbrain showed the co-expression of *chRNA3*<sup>tdTomato</sup>/*mnx1*<sup>eGFP</sup> and *chRNA3*<sup>tdTomato</sup>/*chRNB4*<sup>eGFP</sup>; dashed box region shown magnified for individual transgenic lines; circle shows the location of branchiomotor neurons labeled by *mnx1*<sup>eGFP</sup>. (C–E) Lateral view of the expression of *chRNA3*<sup>tdTomato</sup>, *chRNB4*<sup>eGFP</sup>, and *chRNA5*<sup>tdTomato</sup> positive cells overlapping with *mnx1* expressing cells in motor neurons; dashed box region shown magnified for individual transgenic lines; arrow refers to the overlapped cell; asterisk refers to the motor neuron of *mnx1*<sup>eGFP</sup> positive without the expression of chrn-gene. (F) Quantification of positive cells per segment in the spinal cord in *chRNA3*<sup>tdTomato</sup>, *chRNB4*<sup>eGFP</sup>, and *chRNA5*<sup>tdTomato</sup> crossed with *mnx1*<sup>eGFP/RFP</sup>, *n* = 5 fish for each transgenic line. (G) Quantification of primary motor neurons (pMN) per hemisegment in the spinal cord in *chRNA3*<sup>tdTomato</sup>, *chRNB4*<sup>eGFP</sup>, and *chRNA5*<sup>tdTomato</sup>, *n* = 5 fish for each transgenic line. (H) Transverse view of the expression of *chRNA5*<sup>tdTomato</sup> labeling neurons in the spinal cord and their projections innervated muscles. (H1) Sketch of the projection pattern of the cell that is highly expressed with *chRNA5*<sup>tdTomato</sup> and identified as the sl-type secondary motor neuron. (H2) Lateral view of a cell that highly expressed *chRNA5*<sup>tdTomato</sup>. (I) Lateral view of the co-expression of *chRNB4*<sup>eGFP</sup> and *chRNA5*<sup>tdTomato</sup> in the sl-type secondary motor neuron showed before. Scale bars equal 25  $\mu$ m in (A) and (B), 10  $\mu$ m in (C)–(E), 25  $\mu$ m in (H2) and (I). Quantification data show mean values + standard deviation. C, caudal; D, dorsal; R, rostral.

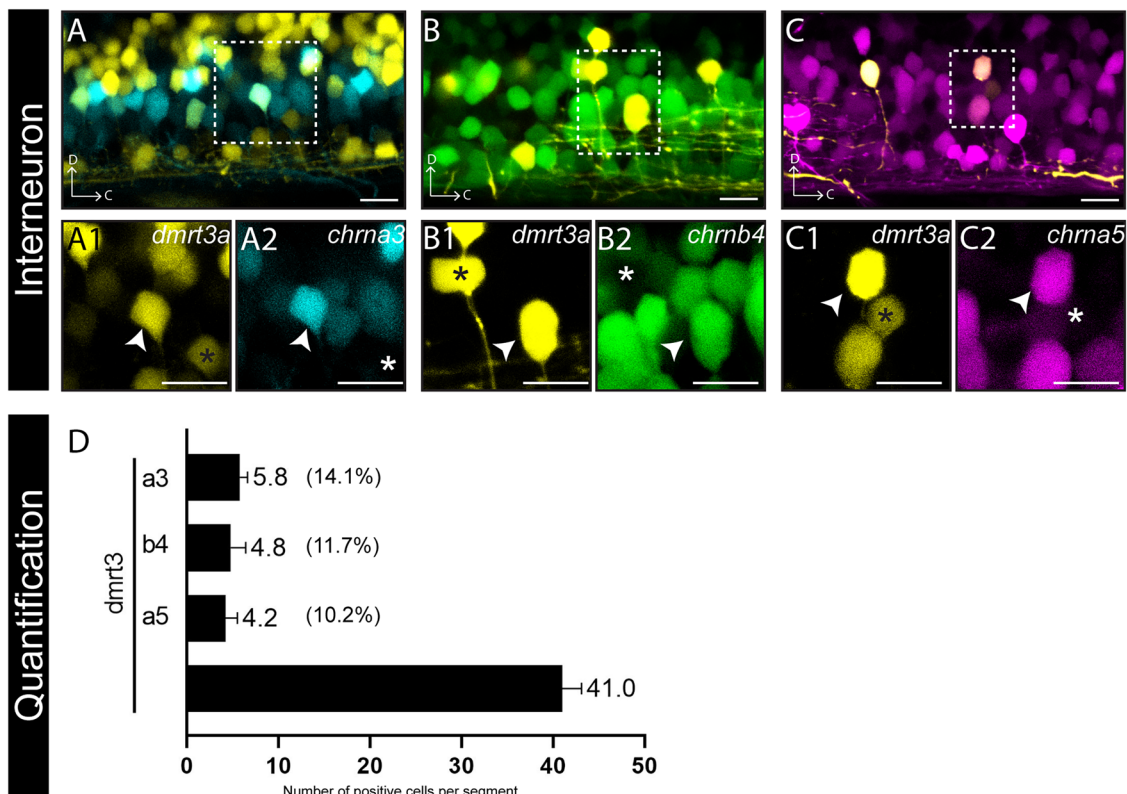


**FIGURE 7** | Expression of *chrna3*<sup>tdTomato</sup>, *chrnb4*<sup>eGFP</sup>, and *chrna5*<sup>tdTomato</sup> in dl6 interneurons. (A–C) Lateral view of the *chrna3*<sup>tdTomato</sup>, *chrnb4*<sup>eGFP</sup>, and *chrna5*<sup>tdTomato</sup> positive cells overlapped with *dmrt3a* expressing cells; dashed box region shown magnified for individual transgenic lines; arrow refers to the overlapped cell; asterisk refers to the interneuron neuron of *dmrt3a*<sup>GFP</sup> positive without the expression of chrn-gene. (D) Quantification of positive cells per segment in the spinal cord in *chrna3*<sup>tdTomato</sup>, *chrnb4*<sup>eGFP</sup>, and *chrna5*<sup>tdTomato</sup> crossed with *dmrt3a*<sup>GFP/RFP</sup>,  $n = 5$  fish for each transgenic line. Scale bars equal 10  $\mu\text{m}$  in (A)–(C), 25  $\mu\text{m}$  in (A1)–(C2). Quantification data show mean values + standard deviation. C, caudal; D, dorsal.

receptor subtypes and eGFP protein may be used to assess overlap within specific cells. Alternatively, single-cell RNA sequencing could reveal the co-expression of the reporter gene and the different chrn-genes within the cells.

As the three chrn-genes examined are closely clustered, there is a chance of reporter leakage through enhancers of the neighboring genes. However, we observed a low degree of co-expression in double chrn-transgenic lines. This suggests little to no ectopic expression as a consequence of their close vicinity, something that may also be verified through single-cell RNA sequencing.

For Tg(*chrnb4*:hs:eGFP) and Tg(*chrna5*:hs:eGFP), we observed a large number of neurons in the spinal cord that expressed low levels of eGFP. In our study, we focused on developmental stages, and it is possible that the observed eGFP is a consequence of transient gene expression following cell fate determination. Further studies exploring expression patterns in the spinal cord of juvenile or adult zebrafish should provide a more accurate picture regarding receptor functionality within the mature network.

#### 4 | Conclusion

In this study, we characterized expressions of Tg(*chrna3*:hs:tdTomato), Tg(*chrnb4*:hs:eGFP), and Tg(*chrna5*:hs:tdTomato) and Tg(*chrna5*:hs:eGFP) zebrafish larvae. Expression was found

in intestine, eye, otic capsule, lateral line, and many areas of the brain, including OB, pineal gland, telencephalon, optic tectum, cerebellum, hindbrain, and spinal cord. For the spinal cord, we predict that 20–39 cells co-express all three genes. Moreover, 23% of neurons expressing *chrna3*<sup>tdTomato</sup> were either motor neurons or *dmrt3a*-expressing inhibitory interneuron. Similarly, 12% of *chrnb4*<sup>eGFP</sup> and 11% of the *chrna5*<sup>tdTomato</sup> populations belonged to these neural subtypes.

Acetylcholine not only acts as a neurotransmitter but also as a neuromodulator (Picciotto, Higley, and Mineur 2012). The distribution of different nAChRs across motor neurons may transfer a difference in response to neuromodulatory ACh exposure. This hypothesis fits in the context of the existence of different speed modules within this network (McLean and Fetcho 2009). For instance, the expression of *chrna7* has been observed in some, but not all, motor neurons (Rima et al. 2020) and interneurons (Iglesias González et al. 2021). Expression of this receptor would thus generate a different response compared to those expressing b4a3(a5)-receptors, when presented with the same concentration of ACh. In addition, the balance among receptor subtypes also determines how cells respond to ACh. We should keep in mind, however, that the restricted expression of *chrna3-b4-a5* genes, that is, only a fraction of the entire population, may lessen the impact of disrupted gene expression on observable locomotor behavior. For instance, if *chrna3-b4-a5* expression is indeed restricted to one of the three speed modules within the locomotor

network, any change in receptor balance may only be visible within that module's given speed range.

Further studies are needed to link expression in the spinal cord to specific speed modules. Assessing the consequences for disrupting receptor subunit balance, for instance, through the generation of (conditional) knock-out animals, may provide insights into the role for a given receptor subunit as well as the functions of the cell expressing it. However, the deletion of a gene may be compensated for during development and change how the network operates. Moreover, deleting a gene from the genome has consequences beyond the locomotor network. For instance, mice lacking the  $\alpha 3$  subunit show impaired growth and an elevated perinatal mortality rate due to developmental abnormalities (Xu et al. 1999). To overcome these challenges, the use of optogenetic tools should be considered, which will allow the silencing of neurons expressing the *chnr*-gene of interest (Koning, Ahemaiti, and Boije 2022). Using fictive locomotion would facilitate the manipulation and measurement of cell activity under different behavioral conditions, thereby providing valuable insights into the functional implications of neurons expressing different subunits in vivo under normal developmental conditions.

#### Author Contributions

**Yuanqi Hua:** experimental design, data acquisition, data interpretation, drafted the manuscript. **Judith Habicher:** experimental design, data acquisition, data interpretation, reviewed the manuscript. **Matthias Carl:** data interpretation, reviewed the manuscript. **Remy Manuel:** experimental design, data acquisition, data interpretation, reviewed the manuscript, supervised the research project, and obtained funding. **Henrik Boije:** experimental design, data interpretation, reviewed the manuscript, supervised the research project, and obtained funding. All authors contributed to the article and approved the submitted version.

#### Acknowledgments

We thank the Zebrafish Core Facility (CIV), Uppsala, Sweden for fish husbandry, and input and exchange of method development. Financial support from: the Kjell and Marta Beijers Foundation; the Jeansson foundation; the Carl Tryggers Foundation; the Swedish Brain Foundation; the Swedish Research Council; the Magnus Bergvalls Foundation, the Royal Swedish Academy of Sciences; the Ake Wibergs Foundation; Olle Engkvist Stiftelse; the Ragnar Söderberg Foundation, Swedish Foundation for Strategic Research, and Swedish Research Council (2015–03359 and 2020-00943).

#### Ethics Statement

The ethics approvals were obtained from the local ethical board in Uppsala (C164/14 and 14088/2019).

#### Conflicts of Interest

The authors declare no conflicts of interest.

#### Data Availability Statement

The raw data supporting the conclusions of this article will be made available by the authors without undue reservation.

#### References

Albuquerque, E. X., E. F. R. Pereira, M. Alkondon, and S. W. Rogers. 2009. "Mammalian Nicotinic Acetylcholine Receptors: From Structure to

Function." *Physiological Reviews* 89, no. 1: 73–120. <https://doi.org/10.1152/physrev.00015.2008>.

Baeza-Loya, S., and D. W. Raible. 2023. "Vestibular Physiology and Function in Zebrafish." *Frontiers in Cell and Developmental Biology* 11: 1172933. <https://doi.org/10.3389/fcell.2023.1172933>.

Bello-Rojas, S., A. E. Istrate, S. Kishore, and D. L. McLean. 2019. "Central and Peripheral Innervation Patterns of Defined Axial Motor Units in Larval Zebrafish." *Journal of Comparative Neurology* 527, no. 15: 2557–2572. <https://doi.org/10.1002/cne.24689>.

Bleckmann, H., and R. Zelig. 2009. "Lateral Line System of Fish." *Integrative Zoology* 4, no. 1: 13–25. <https://doi.org/10.1111/j.1749-4877.2008.00131.x>.

Boije, H., S. Rulands, S. Dudczig, B. D. Simons, and W. A. Harris. 2015. "The Independent Probabilistic Firing of Transcription Factors: A Paradigm for Clonal Variability in the Zebrafish Retina." *Developmental Cell* 34, no. 5: 532–543. <https://doi.org/10.1016/j.devcel.2015.08.011>.

Carlson, A. B., and G. P. Kraus. 2024. *Physiology, Cholinergic Receptors*. Treasure Island (FL): StatPearls Publishing. <http://www.ncbi.nlm.nih.gov/books/NBK526134/>.

Chandrasekhar, A., C. B. Moens, J. T. Warren Jr., C. B. Kimmel, and J. Y. Kuwada. 1997. "Development of Branchiomotor Neurons in Zebrafish." *Development (Cambridge, England)* 124, no. 13: 2633–2644. <https://doi.org/10.1242/dev.124.13.2633>.

Dani, J. A. 2015. "Neuronal Nicotinic Acetylcholine Receptor Structure and Function and Response to Nicotine." *International Review of Neurobiology* 124: 3–19. <https://doi.org/10.1016/bs.irn.2015.07.001>.

Decembrini, S., C. Martin, F. Sennlaub, et al. 2017. "Cone Genesis Tracing by the *Chrn4*-EGFP Mouse Line: Evidences of Cellular Material Fusion After Cone Precursor Transplantation." *Molecular Therapy: The Journal of the American Society of Gene Therapy* 25, no. 3: 634–653. <https://doi.org/10.1016/j.yamthe.2016.12.015>.

DeMarco, E., N. Xu, H. Baier, and E. Robles. 2020. "Neuron Types in the Zebrafish Optic Tectum Labeled by an *id2b* Transgene." *Journal of Comparative Neurology* 528, no. 7: 1173–1188. <https://doi.org/10.1002/cne.24815>.

Dineley-Miller, K., and J. Patrick. 1992. "Gene Transcripts for the Nicotinic Acetylcholine Receptor Subunit,  $\beta 4$ , Are Distributed in Multiple Areas of the Rat Central Nervous System." *Brain Research. Molecular Brain Research* 16, no. 3–4: 339–344. [https://doi.org/10.1016/0169-328x\(92\)90244-6](https://doi.org/10.1016/0169-328x(92)90244-6).

Dwyer, J. B., S. C. McQuown, and F. M. Leslie. 2009. "The Dynamic Effects of Nicotine on the Developing Brain." *Pharmacology & Therapeutics* 122, no. 2: 125–139. <https://doi.org/10.1016/j.pharmthera.2009.02.003>.

Flora, A., R. Schulz, R. Benfante, et al. 2000. "Neuronal and Extraneuronal Expression and Regulation of the Human  $\alpha 5$  Nicotinic Receptor Subunit Gene." *Journal of Neurochemistry* 75, no. 1: 18–27. <https://doi.org/10.1046/j.1471-4159.2000.0750018.x>.

Folgueira, M., C. Sueiro, I. Rodríguez-Moldes, J. Yáñez, and R. Anadón. 2007. "Organization of the Torus Longitudinalis in the Rainbow Trout (*Oncorhynchus mykiss*): An Immunohistochemical Study of the GABAergic System and a DiI Tract-Tracing Study." *Journal of Comparative Neurology* 503, no. 2: 348–370. <https://doi.org/10.1002/cne.21363>.

Förster, D., T. O. Helmbrecht, D. S. Mearns, L. Jordan, N. Mokayes, and H. Baier. 2020. "Retinotectal Circuitry of Larval Zebrafish Is Adapted to Detection and Pursuit of Prey." *Elife* 9: e58596. <https://doi.org/10.7554/eLife.58596>.

Fowler, C. D., Q. Lu, P. M. Johnson, M. J. Marks, and P. J. Kenny. 2011. "Habenular  $\alpha 5$  Nicotinic Receptor Subunit Signalling Controls Nicotine Intake." *Nature* 471, no. 7340: 597–601. <https://doi.org/10.1038/nature09797>.

Frahm, S., M. A. Ślimak, L. Ferrarese, et al. 2011. "Aversion to Nicotine Is Regulated by the Balanced Activity of  $\beta 4$  and  $\alpha 5$  Nicotinic Receptor

- Subunits in the Medial Habenula." *Neuron* 70, no. 3: 522–535. <https://doi.org/10.1016/j.neuron.2011.04.013>.
- Gabashvili, I. S., B. H. A. Sokolowski, C. C. Morton, and A. B. S. Giersch. 2007. "Ion Channel Gene Expression in the Inner Ear." *JARO: Journal of the Association for Research in Otolaryngology* 8, no. 3: 305–328. <https://doi.org/10.1007/s10162-007-0082-y>.
- Garza, A., L. Z. Huang, J. H. Son, and U. H. Winzer-Serhan. 2009. "Expression of Nicotinic Acetylcholine Receptors and Subunit Messenger RNAs in the Enteric Nervous System of the Neonatal Rat." *Neuroscience* 158, no. 4: 1521–1529. <https://doi.org/10.1016/j.neuroscience.2008.11.027>.
- Glick, S. D., I. M. Maisonneuve, B. A. Kitchen, and M. W. Fleck. 2002. "Antagonism of Alpha 3 Beta 4 Nicotinic Receptors as a Strategy to Reduce Opioid and Stimulant Self-Administration." *European Journal of Pharmacology* 438, no. 1–2: 99–105. [https://doi.org/10.1016/S0014-2999\(02\)01284-0](https://doi.org/10.1016/S0014-2999(02)01284-0).
- Grady, S. R., M. Moretti, M. Zoli, et al. 2009. "Rodent Habenulo-Interpeduncular Pathway Expresses a Large Variety of Uncommon nAChR Subtypes, but Only the Alpha3beta4\* and Alpha3beta3beta4\* Subtypes Mediate Acetylcholine Release." *Journal of Neuroscience: The Official Journal of the Society for Neuroscience* 29, no. 7: 2272–2282. <https://doi.org/10.1523/JNEUROSCI.5121-08.2009>.
- Habicher, J., R. Manuel, A. Pedroni, C. Ferebee, K. Ampatzis, and H. Boije. 2022. "A New Transgenic Reporter Line Reveals Expression of Protocadherin 9 at a Cellular Level Within the Zebrafish Central Nervous System." *Gene Expression Patterns: GEP* 44: 119246. <https://doi.org/10.1016/j.gep.2022.119246>.
- Hellström-Lindahl, E., O. Gorbounova, A. Seiger, M. Mousavi, and A. Nordberg. 1998. "Regional Distribution of Nicotinic Receptors During Prenatal Development of Human Brain and Spinal Cord." *Brain Research. Developmental Brain Research* 108, no. 1–2: 147–160. [https://doi.org/10.1016/S0165-3806\(98\)00046-7](https://doi.org/10.1016/S0165-3806(98)00046-7).
- Holbrook, B. D. 2016. "The Effects of Nicotine on Human Fetal Development." *Birth Defects Research. Part C, Embryo Today: Reviews* 108, no. 2: 181–192. <https://doi.org/10.1002/bdrc.21128>.
- Iglesias González, A. B., J. E. T. Jakobsson, J. Vieillard, M. C. Lagerström, K. Kullander, and H. Boije. 2021. "Single Cell Transcriptomic Analysis of Spinal Dmrt3 Neurons in Zebrafish and Mouse Identifies Distinct Subtypes and Reveal Novel Subpopulations Within the dl6 Domain." *Frontiers in Cellular Neuroscience* 15: 781197. <https://doi.org/10.3389/fncel.2021.781197>.
- Iglesias Gonzalez, A. B., H. K. Koning, M. U. Tuz-Sasik, I. van Osselen, R. Manuel, and H. Boije. 2024. "Perturbed Development of Calb2b Expressing dl6 Interneurons and Motor Neurons Underlies Locomotor Defects Observed in Calretinin Knock-Down Zebrafish Larvae." *Developmental Biology* 508: 77–87. <https://doi.org/10.1016/j.ydbio.2024.01.001>.
- Improgo, M. A. R. D., M. D. Scofield, A. R. Tapper, and P. D. Gardner. 2010. "The Nicotinic Acetylcholine Receptor CHRNA5/A3/B4 Gene Cluster: Dual Role in Nicotine Addiction and Lung Cancer." *Progress in Neurobiology* 92, no. 2: 212–226. <https://doi.org/10.1016/j.pneurobio.2010.05.003>.
- Kalamida, D., K. Poulas, V. Avramopoulou, et al. 2007. "Muscle and Neuronal Nicotinic Acetylcholine Receptors." *FEBS Journal* 274, no. 15: 3799–3845. <https://doi.org/10.1111/j.1742-4658.2007.05935.x>.
- Kamens, H. M., C. S. McKinnon, N. Li, M. L. Helms, J. K. Belknap, and T. J. Phillips. 2009. "The  $\alpha 3$  Subunit Gene of the Nicotinic Acetylcholine Receptor Is a Candidate Gene for Ethanol Stimulation." *Genes, Brain, and Behavior* 8, no. 6: 600–609. <https://doi.org/10.1111/j.1601-183X.2008.00444.x>.
- Kimura, Y., Y. Hisano, A. Kawahara, and S.-i. Higashijima. 2014. "Efficient Generation of Knock-in Transgenic Zebrafish Carrying Reporter/Driver Genes by CRISPR/Cas9-Mediated Genome Engineering." *Scientific Reports* 4, no. 1: 6545. <https://doi.org/10.1038/srep06545>.
- Koning, H. K., A. Ahemaiti, and H. Boije. 2022. "A Deep-Dive Into Fictive Locomotion—A Strategy to Probe Cellular Activity During Speed Transitions in Fictively Swimming Zebrafish Larvae." *Biology Open* 11, no. 3: bio059167. <https://doi.org/10.1242/bio.059167>.
- Kuil, L. E., R. K. Chauhan, W. W. Cheng, R. M. W. Hofstra, and M. M. Alves. 2021. "Zebrafish: A Model Organism for Studying Enteric Nervous System Development and Disease." *Frontiers in Cell and Developmental Biology* 8: 629073.
- LaMora, A., and M. M. Voigt. 2009. "Cranial Sensory Ganglia Neurons Require Intrinsic N-Cadherin Function for Guidance of Afferent Fibers to Their Final Targets." *Neuroscience* 159, no. 3: 1175–1184. <https://doi.org/10.1016/j.neuroscience.2009.01.049>.
- Lee, S.-H.a, E. S. Barrie, W. Sadee, and R. M. Smith. 2019. "Nicotine Dependence and the CHRNA5/CHRNA3/CHRNA4 Nicotinic Receptor Regulome." In *Neuroscience of Nicotine*, edited by V. R. Preedy, 347–353. Cambridge: Academic Press. <https://www.sciencedirect.com/science/article/pii/B9780128130353000435>.
- Lein, E. D. S., M. J. Hawrylycz, N. Ao, et al. 2007. "Genome-Wide Atlas of Gene Expression in the Adult Mouse Brain." *Nature* 445, no. 7124: 168–176. <https://doi.org/10.1038/nature05453>.
- Li, X., J. Montgomery, W. Cheng, J. H. Noh, D. R. Hyde, and L. Li. 2012. "Pineal Photoreceptor Cells Are Required for Maintaining the Circadian Rhythms of Behavioral Visual Sensitivity in Zebrafish." *PLoS ONE* 7, no. 7: e40508. <https://doi.org/10.1371/journal.pone.0040508>.
- Manuel, R., A. B. Iglesias Gonzalez, J. Habicher, H. K. Koning, and H. Boije. 2021. "Characterization of Individual Projections Reveal That Neuromasts of the Zebrafish Lateral Line Are Innervated by Multiple Inhibitory Efferent Cells." *Frontiers in Neuroanatomy* 15: 666109. <https://doi.org/10.3389/fnana.2021.666109>.
- McGehee, D. S., and L. W. Role. 1995. "Physiological Diversity of Nicotinic Acetylcholine Receptors Expressed by Vertebrate Neurons." *Annual Review of Physiology* 57, no. 1: 521–546. <https://doi.org/10.1146/annurev.ph.57.030195.002513>.
- McLean, D. L., and J. R. Fetcho. 2009. "Spinal Interneurons Differentiate Sequentially From Those Driving the Fastest Swimming Movements in Larval Zebrafish to Those Driving the Slowest Ones." *Journal of Neuroscience: The Official Journal of the Society for Neuroscience* 29, no. 43: 13566–13577. <https://doi.org/10.1523/JNEUROSCI.3277-09.2009>.
- Moretti, M., S. Vailati, M. Zoli, et al. 2004. "Nicotinic Acetylcholine Receptor Subtypes Expression During Rat Retina Development and Their Regulation by Visual Experience." *Molecular Pharmacology* 66, no. 1: 85–96. <https://doi.org/10.1124/mol.66.1.85>.
- Patthey, C., H. Clifford, W. Haerty, C. P. Ponting, S. M. Shimeld, and J. O. Begbie. 2016. "Identification of Molecular Signatures Specific for Distinct Cranial Sensory Ganglia in the Developing Chick." *Neural Development* 11, no. 1: 3. <https://doi.org/10.1186/s13064-016-0057-y>.
- Perry, D. C., Y. Xiao, H. N. Nguyen, J. L. Musachio, M. I. Dávila-García, and K. J. Kellar. 2002. "Measuring Nicotinic Receptors With Characteristics of Alpha4beta2, Alpha3beta2 and Alpha3beta4 Subtypes in Rat Tissues by Autoradiography." *Journal of Neurochemistry* 82, no. 3: 468–481. <https://doi.org/10.1046/j.1471-4159.2002.00951.x>.
- Piccio, M. R., M. J. Higley, and Y. S. Mineur. 2012. "Acetylcholine as a Neuromodulator: Cholinergic Signaling Shapes Nervous System Function and Behavior." *Neuron* 76, no. 1: 116–129. <https://doi.org/10.1016/j.neuron.2012.08.036>.
- Raimondi, E., F. Rubboli, D. Moralli, et al. 1992. "Chromosomal Localization and Physical Linkage of the Genes Encoding the Human Alpha 3, Alpha 5, and Beta 4 Neuronal Nicotinic Receptor Subunits." *Genomics* 12, no. 4: 849–850. [https://doi.org/10.1016/0888-7543\(92\)90324-1](https://doi.org/10.1016/0888-7543(92)90324-1).
- Rima, M., Y. Lattouf, M. Abi Younes, et al. 2020. "Dynamic Regulation of the Cholinergic System in the Spinal Central Nervous System." *Scientific Reports* 10, no. 1: 15338. <https://doi.org/10.1038/s41598-020-72524-3>.
- Rueda Ruzafa, L., J. L. Cedillo, and A. J. Hone. 2021. "Nicotinic Acetylcholine Receptor Involvement in Inflammatory Bowel Disease and Interactions With Gut Microbiota." *International Journal of Environmental*

- Research and Public Health 18, no. 3: 1189. <https://doi.org/10.3390/jerph18031189>.
- Sabatelli, M., F. Eusebi, A. Al-Chalabi, et al. 2009. "Rare Missense Variants of Neuronal Nicotinic Acetylcholine Receptor Altering Receptor Function Are Associated With Sporadic Amyotrophic Lateral Sclerosis." *Human Molecular Genetics* 18, no. 20: 3997–4006. <https://doi.org/10.1093/hmg/ddp339>.
- Saccone, N. L., J. C. Wang, N. Breslau, et al. 2009. "The CHRNA5-CHRNA3-CHRNA4 Nicotinic Receptor Subunit Gene Cluster Affects Risk for Nicotine Dependence in African-Americans and in European-Americans." *Cancer Research* 69, no. 17: 6848–6856. <https://doi.org/10.1158/0008-5472.CAN-09-0786>.
- Satou, C., Y. Kimura, H. Hirata, M. L. Suster, K. Kawakami, and S.-i. Higashijima. 2013. "Transgenic Tools to Characterize Neuronal Properties of Discrete Populations of Zebrafish Neurons." *Development (Cambridge, England)* 140, no. 18: 3927–3931. <https://doi.org/10.1242/dev.099531>.
- Scofield, M. D., A. R. Tapper, and P. D. Gardner. 2010. "A Transcriptional Regulatory Element Critical for CHRNA4 Promoter Activity In Vivo." *Neuroscience* 170, no. 4: 1056–1064. <https://doi.org/10.1016/j.neuroscience.2010.08.007>.
- Seredick, S. D., L. Van Ryswyk, S. A. Hutchinson, and J. S. Eisen. 2012. "Zebrafish Mnx Proteins Specify One Motoneuron Subtype and Suppress Acquisition of Interneuron Characteristics." *Neural Development* 7: 35. <https://doi.org/10.1186/1749-8104-7-35>.
- Shainer, I., A. Buchshtab, T. A. Hawkins, S. W. Wilson, R. D. Cone, and Y. Gothilf. 2017. "Novel Hypophysiotropic AgRP2 Neurons and Pineal Cells Revealed by BAC Transgenesis in Zebrafish." *Scientific Reports* 7: 44777. <https://doi.org/10.1038/srep44777>.
- Shrestha, B. R., C. Chia, L. Wu, S. G. Kujawa, M. C. Liberman, and L. V. Goodrich. 2018. "Sensory Neuron Diversity in the Inner Ear Is Shaped by Activity." *Cell* 174, no. 5: 1229–1246.e17. <https://doi.org/10.1016/j.cell.2018.07.007>.
- Stella, N., and D. Piomelli. 2001. "Receptor-Dependent Formation of Endogenous Cannabinoids in Cortical Neurons." *European Journal of Pharmacology* 425, no. 3: 189–196. [https://doi.org/10.1016/s0014-2999\(01\)01182-7](https://doi.org/10.1016/s0014-2999(01)01182-7).
- Stolerman, I. P., N. R. Mirza, B. Hahn, and M. Shoaib. 2000. "Nicotine in an Animal Model of Attention." *European Journal of Pharmacology* 393, no. 1–3: 147–154. [https://doi.org/10.1016/s0014-2999\(99\)00886-9](https://doi.org/10.1016/s0014-2999(99)00886-9).
- Sur, A., Y. Wang, P. Capar, G. Margolin, and J. A. Farrell. 2023. "Single-Cell Analysis of Shared Signatures and Transcriptional Diversity During Zebrafish Development." *Developmental Cell* 58, no. 24: 3028–3047.e12. <https://doi.org/10.1016/j.devcel.2023.11.001>.
- Svoboda, K. R., S. Vijayaraghavan, and R. L. Tanguay. 2002. "Nicotinic Receptors Mediate Changes in Spinal Motoneuron Development and Axonal Pathfinding in Embryonic Zebrafish Exposed to Nicotine." *Journal of Neuroscience* 22, no. 24: 10731–10741. <https://doi.org/10.1523/JNEUROSCI.22-24-10731.2002>.
- Takahashi, T. 2020. "Roles of nAChR and Wnt Signaling in Intestinal Stem Cell Function and Inflammation." *International Immunopharmacology* 81: 106260. <https://doi.org/10.1016/j.intimp.2020.106260>.
- Thisse, C., and B. Thisse. 2008. "High-Resolution In Situ Hybridization to Whole-Mount Zebrafish Embryos." *Nature Protocols* 3, no. 1: 59–69. <https://doi.org/10.1038/nprot.2007.514>.
- Varshney, G. K., W. Pei, M. C. LaFave, et al. 2015. "High-Throughput Gene Targeting and Phenotyping in Zebrafish Using CRISPR/Cas9." *Genome Research* 25, no. 7: 1030–1042. <https://doi.org/10.1101/gr.186379.114>.
- Wang, F., V. Gerzanich, G. B. Wells, et al. 1996. "Assembly of Human Neuronal Nicotinic Receptor Alpha5 Subunits With Alpha3, Beta2, and Beta4 Subunits." *The Journal of Biological Chemistry* 271, no. 30: 17656–17665. <https://doi.org/10.1074/jbc.271.30.17656>.
- Winzer-Serhan, U. H., and F. M. Leslie. 1997. "Codistribution of Nicotinic Acetylcholine Receptor Subunit Alpha3 and Beta4 mRNAs During Rat Brain Development." *Journal of Comparative Neurology* 386, no. 4: 540–554. [https://doi.org/10.1002/\(sici\)1096-9861\(19971006\)386:4\(540::aid-cne2\)3.0.co;2-2](https://doi.org/10.1002/(sici)1096-9861(19971006)386:4(540::aid-cne2)3.0.co;2-2).
- Xu, W., S. Gelber, A. Orr-Urtreger, et al. 1999. "Megacystis, Mydriasis, and Ion Channel Defect in Mice Lacking the Alpha3 Neuronal Nicotinic Acetylcholine Receptor." *Proceedings of the National Academy of Sciences of the United States of America* 96, no. 10: 5746–5751. <https://doi.org/10.1073/pnas.96.10.5746>.
- Xu, X., M. M. Scott, and E. S. Deneris. 2006. "Shared Long-Range Regulatory Elements Coordinate Expression of a Gene Cluster Encoding Nicotinic Receptor Heteromeric Subtypes." *Molecular and Cellular Biology* 26, no. 15: 5636–5649. <https://doi.org/10.1128/MCB.00456-06>.
- Yang, X., X. Guo, Z. Huang, et al. 2019. "CHRNA5/CHRNA3 Gene Cluster Is a Risk Factor for Lumbar Disc Herniation: A Case-Control Study." *Journal of Orthopaedic Surgery and Research* 14: 243. <https://doi.org/10.1186/s13018-019-1254-2>.
- Zoli, M., N. Le Novère, J. A. Hill, and J. P. Changeux. 1995. "Developmental Regulation of Nicotinic ACh Receptor Subunit mRNAs in the Rat Central and Peripheral Nervous Systems." *Journal of Neuroscience: The Official Journal of the Society for Neuroscience* 15, no. (3 pt. 1): 1912–1939.
- Zoli, M., F. Pistillo, and C. Gotti. 2015. "Diversity of Native Nicotinic Receptor Subtypes in Mammalian Brain." *Neuropharmacology* 96, no. Pt B: 302–311. <https://doi.org/10.1016/j.neuropharm.2014.11.003>.

### Supporting Information

Additional supporting information can be found online in the Supporting Information section.